Published in final edited form as:
J Control Release. 2007 April 23; 118(3): 285–293.

Ultrasonically targeted delivery into endothelial and smooth muscle cells in *ex vivo* arteries

Daniel M. Hallow, **Anuj D. Mahajan**, and **Mark R. Prausnitz**
School of Chemical & Biomolecular Engineering, Georgia Institute of Technology, Atlanta, GA 30332, USA.

Abstract

This study tested the hypothesis that ultrasound can target intracellular uptake of drugs into vascular endothelial cells (ECs) at low to intermediate energy and into smooth muscle cells (SMCs) at high energy. Ultrasound-enhanced delivery has been shown to enhance and target intracellular drug and gene delivery in the vasculature to treat cardiovascular disease, but quantitative studies of the delivery process are lacking. Viable *ex vivo* porcine carotid arteries were placed in a solution containing a model drug, TO-PRO®-1, and Optison® microbubbles. Arteries were exposed to ultrasound at 1.1 MHz and acoustic energies of 5.0, 66, or 630 J/cm^2. Using confocal microscopy and fluorescent labeling of cells, the artery endothelium and media were imaged to determine the localization and to quantify intracellular uptake and cell death. At low to intermediate ultrasound energy, ultrasound was shown to target intracellular delivery into viable cells that represented 9 – 24% of exposed ECs. These conditions also typically caused 7 – 25% EC death. At high energy, intracellular delivery was targeted to SMCs, which was associated with denuding or death of proximal ECs. This work represents the first known in-depth study to evaluate intracellular uptake into cells in tissue. We conclude that significant intracellular uptake of molecules can be targeted into ECs and SMCs by ultrasound-enhanced delivery suggesting possible applications for treatment of cardivascular diseases and dysfunctions.

Keywords

ultrasound; cavitation; intracellular drug delivery; endothelial cells; targeted drug delivery

INTRODUCTION

Cardiovascular disease is one of the leading causes of death worldwide, resulting in nearly 17 million deaths annually [1]. Targeted drug and gene delivery to vascular endothelial cells (ECs) and smooth muscle cells (SMCs) has increasingly become a focus for treating cardiovascular diseases and dysfunctions, such as coronary artery disease, hypercholesterolemia, hypertension, and restenosis, because of the pivotal role of these cells in controlling and maintaining vascular functions [2–4]. In addition, targeted drug and gene delivery to the endothelium is being used to treat cancerous tumors by anti-vascular therapy [5] and myocardial and peripheral ischemia by promoting angiogenesis [6]. Many drug and gene delivery systems are being developed to increase targeting to vascular cells, such as drug-

Address for correspondence Mark Prausnitz, School of Chemical & Biomolecular Engineering, Georgia Institute of Technology, 311 Ferst Drive, Atlanta, GA 30332-0100, USA, Phone: (404) 385-5135, Fax: (404) 894-2291, E-mail: prausnitz@gatech.edu

eluting stents [7], catheter-based systems [8], viral vectors [9,10], and targeted liposomes [11] and microbubbles [12]. However, most current techniques lack either the effectiveness or specificity to adequately treat these disorders while safely administering the therapeutic and avoiding toxic systemic effects or require significantly invasive intervention. A safe, effective, and non-invasive method to target delivery of drugs or genes to the specific disease site in the vasculature would greatly benefit cardiovascular treatments.

A novel approach to targeting drug and gene administration is the method of ultrasound-enhanced delivery [13–15]. Ultrasound-enhanced delivery often exploits cavitation bubble activity, which can be produced by the pressure oscillations of ultrasound [16]. Furthermore, ultrasound pressures above a certain threshold can cause oscillating bubbles to undergo violent collapse known as inertial cavitation [17]. Inertial cavitation is believed to cause transient disruptions in cell membranes, enabling transport of extracellular molecules (e.g., drugs or genes) into viable cells [18–20]. Cavitation-mediated cellular disruptions can allow uptake of small molecules, macromolecules (e.g., proteins), and genetic material (e.g., plasmid DNA or siRNA). Furthermore, ultrasound-enhanced delivery has been studied in a variety of *in vitro* and *in vivo* scenarios and has demonstrated promising therapeutic results after intracellular uptake of drugs and gene expression [14,16,21]. Most importantly, ultrasound can be targeted in the body by non-invasive extracorporeal focused ultrasound [22] or by minimally invasive catheter-based transducers [23]. Greater efficacy and reduced side effects could be realized by this targeted therapy.

The vascular endothelium is an attractive target for ultrasound-enhanced delivery because cavitation can be readily produced in the vasculature, which currently occurs to a mild extent during diagnostic imaging [24]. Moreover, cavitation is expected to have limited effects beyond cell layers directly experiencing cavitation activity, and the endothelium is the first point of contact to cavitation activity [25]. A number of researchers are currently studying ultrasound-enhanced gene therapy for cardiovascular disorders in order to control intimal hyperplasia, restore vascular function, or promote angiogenesis [21]. These studies have shown expression of reporter plasmids as well as plasmids with a therapeutic purpose. Clinical potential of this method has been shown by causing protein expression by plasmid DNA [26] or blocking specific proteins by oligonucleotides [27].

A recognized limitation of ultrasound-enhanced delivery is the need for more cells with drug uptake or gene expression [21]. Many studies have demonstrated gene transfection and tissue response in *ex vivo* and *in vivo* systems; however, few studies have been directed at quantifying the intracellular uptake of molecules and imaging bioeffects (i.e., intracellular uptake and loss of viability) caused by ultrasound-enhanced delivery in viable tissue [16,28]. It is important to know the uptake efficiency at different ultrasound energies in order to design and apply this technique for drug or gene delivery applications. In this study, we sought to determine whether ultrasound-enhanced delivery of a model drug can be targeted into ECs and SMCs in *ex vivo* arteries. This work represents the first known in-depth study to quantify and image the intracellular uptake of molecules and loss of viability to vascular cells by ultrasound-enhanced delivery. We hypothesize that ultrasound can target intracellular uptake of drugs into the vascular endothelium at low to intermediate energy and into SMCs at high energy. To assess this hypothesis, our goals in this study were to image the localization of (i) intracellular uptake of a model drug and (ii) loss of viability to vascular cells and (iii) to specifically quantify endothelial bioeffects in the targeted region.

METHODS

Porcine Carotid Artery Isolation and Preparation

Porcine carotid arteries were chosen for this study because they can be delicately excised without tissue damage, preserving an intact and viable endothelium. Furthermore, carotid arteries are relatively straight vessels without much branching, simplifying handling and imaging of the artery. Porcine carotid arteries were harvested from freshly killed female swine at a local abattoir (Holifield Farms, Convington, GA). Excised arteries were immediately rinsed with sterile phosphate-buffered saline (PBS, MediaTech, Herndon, VA) and placed in 15-ml conical tubes filled with Dulbecco's Modified Eagle Medium (DMEM, MediaTech) supplemented with 100 μg/ml penicillin-streptomycin (MediaTech) and 10% (v/v) heat-inactivated fetal bovine serum (Atlanta Biologicals, Atlanta, GA). Arteries were then placed on ice for approximately 1 h during transport to the laboratory. Upon return to the laboratory, arteries were placed in fresh DMEM with 15 μM sodium nitroprusside (Sigma, St. Louis, MO) and incubated at 37°C for approximately 30 min while the ultrasound apparatus was prepared. Sodium nitroprusside, a nitric oxide donor, was added to the media to relax the arteries, improving the *en face* images of the artery (as described below). Arteries were then cleaned of adventitial adipose and connective tissue while submerged in DMEM.

Flat Artery Experiments

To prepare flat arteries for simplified exposure and analysis, the ends of the intact arteries were first discarded where the artery was handled with forceps, which likely caused tissue damage. Arteries were then cut cross-sectionally into 1-cm length segments and cut lengthwise to expose the endothelial surface. To approximate physiologic tension, artery segments were stretched to ~150% of their resting length [29], sutured to acoutically transparent TPX® plastic disks (25 mm dia., Ajedium Film, Newark, DE) with the endothelium exposed (Fig. 1), submerged in DMEM, and incubated at 37°C. In select experiments, the artery endothelium was removed by rubbing the endothelial surface with a plastic cell scraper (Becton Dickinson, Franklin Lakes, NJ) denuding the artery completely, as verified by microscopy.

Intact Artery Experiments

To better mimic the *in vivo* geometry and environment, intact arteries were cut into 2.5-cm length segments and cannulated on each end in custom-built chambers for ultrasound exposure. Chambers were rectangular-shaped boxes constructed of acrylic plastic with metal cannulas on each end to suspend the artery lengthwise and acoustically transparent windows constructed of Mylar® (DuPont, Wilmington, DE) plastic to allow ultrasound exposure with minimal attenuation. Physiologic stretch and pressure were obtained by stretching the artery by ~150% and pressurizing the artery with DMEM or blood to 100 mmHg. The volume outside the artery was filled with DMEM, and then the chamber was incubated at 37°C.

Ultrasound Apparatus

Ultrasound was produced using an immersible, focused, piezoceramic transducer (Sonic Concepts, Woodinville, WA, model no. H-101) at 1.1 MHz. The transducer had a 70-mm diameter, 52-mm focal length, and 1.5-mm focal width at half amplitude (−6 dB). Megahertz ultrasound was used in this study because frequencies in the vicinity of 1.1 MHz have been well established in our lab and many others to nucleate microbubbles and cause intracellular uptake of drugs and genes [16]. Megahertz ultrasound is widely studied because it can be highly focused and is considered safer than lower frequencies, since it is less likely to spontaneously produce cavitation. Therefore, cavitation caused by megahertz ultrasound is enhanced by microbubbles to nucleate cavitation and thereby adds another element of control by allowing one to also regulate cavitation by the microbubbles added to the system.

A sinusoidal waveform was produced by two function generators (Standford Research Instruments, Sunnyvale, CA, model no. DS345 and Agilent, Austin, TX, model no. 33120A) used in conjunction to control pulse length, frequency and peak-to-peak voltage. The sinusoidal waveform was amplified by a RF broadband power amplifier (Electronic Navigation Industries, Rochester, NY, model no. 3100LA) before passing through a matching impedance network and controlling the response of the transducer.

The transducer was housed in a polycarbonate tank (30.5 × 29 × 37 cm) containing approximately 26 L of deionized and distilled water at 37°C. A 5-cm thick acoustic absorber (SC-501 Acoustic Rubber, Sonic Concepts) was mounted opposite the transducer to minimize standing wave formation. A three-axis positioning system (10 μm resolution, Velmex, Bloomfield, NY) was mounted on top of the tank to position samples and a hydrophone at desired locations in the tank. A PVDF membrane hydrophone (NTR Systems, Seattle, WA, model no. MHA200A) was used to measure spatial-peak-temporal-peak negative pressure in order to map and calibrate the acoustic field produced by the transducer.

Experimental Protocol

Prior to every experiment, the desired sample placement in the acoustic field was found by using a needle hydrophone (NTR Systems, model no. TNU001A). The ultrasound beam focus at 1.1 MHz had a focal-width at half-amplitude equal to 1.5 mm, which only allowed a small region of the artery to be exposed. To administer ultrasound to a larger portion of the artery, samples were placed in a location approximately 1 cm out of the ultrasound's focus towards the transducer, which had a focal-width at half-amplitude equal to 10.4 mm.

Prior to ultrasound exposure, a solution for each sample was prepared with DMEM, 4 μM TO-PRO®-1 (Invitrogen, Molecular Probes, Eugene, OR), and 1.7% v/v (~ 1.1×10^7 bubble/ml) Optison® (Mallinckrodt, St. Louis, MO). TO-PRO®-1, a green fluorescent nucleic acid stain that is impermeable to intact cell membranes, was used as a model drug and to quantify intracellular uptake into viable cells. TO-PRO®-1 emits little fluorescence until it binds to nucleic acids inside cells, which facilitates analysis by confocal microscopy by almost eliminating background noise from extracellular TO-PRO®-1. In select intact artery experiments, whole porcine blood, collected from the abattoir, with 5 USP units/ml of heparin (Baxter, Deerfield, IL) was used in place of DMEM to further imitate physiologic conditions.

Optison® is a suspension of perfluorcarbon gas bubbles stabilized with denatured human albumin that is a FDA-approved ultrasound imaging contrast agent but was used in this study to nucleate cavitation activity [30]. Optison® bubbles of mean diameter 3–5 μm are expected to have a resonant frequency of ~2 MHz and a peak negative pressure threshold for inertial cavitation of ~0.4 MPa at 1.1 MHz [17]. Optison® is considered unstable when exposed to air and can be difficult to keep in a homogenous suspension due to buoyancy of the bubbles. Therefore, Optison® was only added immediately before ultrasound exposure. During long ultrasound exposure, intense mixing caused by cavitation activity was expected to keep the solution homogenous. It is envisioned that microbubbles of the relatively high concentrations used in this study could be obtained in the body by local catheter release of microbubbles [23] or by targeted microbubbles [14,31].

Flat arteries were placed in cylindrical sample chambers that had the ends sealed with acoustically transparent TPX® plastic. Immediately before ultrasound exposure, sample chambers containing flat arteries were filled with a sample solution of media, model drug, and Optison®. Intact arteries were filled with the sample solution to physiologic pressure (~100 mmHg). Sample chambers were then placed in the desired location in the ultrasound apparatus using the three-axis positioning system to orient the flat artery surface and the intact artery

segment perpendicular to the acoustic beam. The endothelium was placed facing the transducer in the flat artery experiments.

Ultrasound was applied to each sample at 1.1 MHz and acoustic energies of 5.0 (0.7 MPa – 300 ms), 66 (1.4 MPa – 1000 ms), or 630 J/cm^2 (2.5 MPa – 3000 ms), referred to as low, intermediate, and high ultrasound energy, respectively. To avoid heating, ultrasound was applied in 1-ms bursts followed by 99 ms of off time, a 1% duty cycle. The experimental and acoustic parameters used for this study were based on previous work with cells in suspension showing which conditions caused the range of interesting effects [32]. Inertial cavitation production during ultrasound exposure was verified using a passive cavitation detection system. This system consisted of a focused hydrophone and a high-speed digitizer to record cavitation emissions, as described previously [32]. Recordings of cavitation emissions were processed to derive frequency spectra and allowed monitoring of the broadband noise, an established measure of inertial cavitation [33]. Cavitation detection further showed that cavitation activity was sustained for a series bursts equivalent to several hundreds of milliseconds of ultrasound exposure. After ultrasound exposure, samples were immediately incubated at 37°C for 15 min to allow arteries to "recover", as membrane resealing is expected to occur on the order of a few minutes [19]. Arteries were then rinsed with DMEM and incubated at 37°C for < 20 min until all samples had been exposed.

After ultrasound exposure, intact arteries were removed from their chambers, cut open lengthwise and sutured to rectangular TPX® plastic slides exposing the endothelium. Artery segments were then placed in DMEM with 0.07 mg/ml Hoechst 33342 (Invitrogen) and 7 μg/ml propidium iodide (Invitrogen) for 30 min in the incubator. Hoechst 33342 stains the nuclei of all cells with blue fluorescence, while propidium iodide only stains the nuclei of non-viable cells with red fluorescence.

Microscopy

Artery segments were observed using a Zeiss LSM 510 confocal laser-scanning microscope or Zeiss LSM META/NLO 510 multiphoton microscope (Zeiss, Thornwood, NY). Images of the endothelium and media were captured by directing a 40X magnification oil objective or a 10X magnification objective at the endothelial surface of the artery. To grasp the extent and pattern of the bioeffects, a larger area of the endothelium was captured by taking four overlapping confocal images at 10X magnification and arranging them as a montage.

Quantification and statistical analysis

Quantification of endothelial bioeffects was objectively determined by capturing 20 images at specific locations relative to suturing holes that affixed the artery to the plastic disk. Twenty images of the artery endothelium were captured in a 5 by 4 array at 40X magnification for each sample of the flat artery experiments (Fig. 1). Images were then processed in Image-Pro® Plus (Media Cybernetics, Silver Spring, MD) to count all ECs (blue florescence), non-viable cells (red fluorescence), and viable cells with model drug uptake (green fluorescence). The number of detached ECs from the artery surface of each exposed sample was determined by subtracting the number of remaining intact ECs from the total number of intact ECs of a control sample, which was taken to represent the number cells present prior to ultrasound exposure. Typical control samples would contain at least 4,000 ECs. The number of cells for each population was averaged for each energy and normalized to the control sample. Controls were samples that underwent a sham exposure, i.e., tissue treated identically to other samples except it was not exposed to ultrasound.

Statistical analysis was performed by use of Paired Student's t-Tests and analysis of variance (ANOVA) on quantified bioeffects from flat artery experiments. Values of $P < 0.05$ were considered statistically significant.

RESULTS

Endothelial Bioeffects

To test the hypothesis that ultrasound-mediated cavitation can cause intracellular uptake into ECs, we exposed *ex vivo* arterial segments to ultrasound at three different acoustic energies - termed low, intermediate, and high - and compared these tissues to control artery segments without ultrasound exposure (i.e., sham exposure). Figure 2 displays representative *en face* images of the endothelium of a control tissue and a tissue exposed to ultrasound at the intermediate energy. ECs are recognized by their rounded nuclei morphology and orientation parallel to the direction of blood flow.

Figure 2A1–A2 displays the endothelium of a representative control sample. The control artery appears to have a complete endothelium with high viability, as indicated by the continuum of ECs stained with blue fluorescent Hoechst 33342 (Fig. 2A1) and few ECs stained with red fluorescent propidium iodide (Fig. 2A2). None of the viable ECs appears to have green fluorescent TOPRO-1 staining, verifying that TOPRO-1 was membrane impermeable. These images indicate that arteries were isolated and handled in a manner that retained an intact endothelium and sustained the viability of the artery over the course of the experiment.

We next investigated if ultrasound caused intracellular uptake in the endothelium. Figure 2B1–B2 displays the endothelium of a representative artery exposed to ultrasound at intermediate energy. Fluorescently green stained ECs observed in the exposed sample (Fig. 2B2) clearly indicate intracellular uptake of the model drug, TO-PRO®-1. Since propidium iodide stains any dead or permeable cells, the lack of propidium iodide staining in green ECs indicates that these cells were reversibly permeabilized and remained viable. Thus, we conclude that ultrasound exposure significantly increased intracellular uptake into ECs.

We also observed that intracellular uptake appeared in a pattern of discreet regions or "patches" of fluorescently green nuclei on the surface of the artery (Fig. 2B2). This localized pattern of intracellular uptake was regularly seen in tissues exposed to ultrasound. We expect these regions of uptake can be explained by considering the cavitation-mediated mechanism causing bioeffects. It is commonly believed that bioeffects observed by this technique are due to discreet cavitation events and are heterogeneous within a sample due to the stochastic nature of cavitation. Similar patterns of discreet regions of bioeffects have been observed in *in vitro* monolayers of cells exposed to ultrasound-mediated cavitation and attributed to individual cavitation events occurring near the surface of the monolayer [34,35]. We therefore hypothesize that intracellular uptake is caused by many individual cavitation events occurring near the surface of the artery and creates the observed scattered patches of intracellular uptake in the targeted region of the artery.

In addition to intracellular uptake, we also sought to assess the extent to which ultrasound exposure caused loss of cell viability. In Fig. 2B2, a decrease in viability of the exposed sample was observed, as shown by an increase in the number of fluorescently red nuclei compared to the control sample (Fig. 2A2). This indicates ultrasound exposure can cause EC death.

Guided by the general findings in Fig. 2, we wanted to assess endothelial bioeffects of intracellular uptake and loss of viability in greater detail at different ultrasound energies. In Fig. 3, representative confocal images of control samples and samples exposed at low, intermediate, and high ultrasound energies are shown at two different magnifications. The

extent of bioeffects appears to sharply increase with increasing ultrasound energy. The bioeffects ranged from (i) little intracellular uptake or cell death at the lowest energy (Fig. 3C–D) to (ii) widespread intracellular uptake and reduced viabilities at the intermediate energy (Fig. 3E–F) to (iii) widespread denuding of the endothelium and cell death at the highest ultrasound energy (Fig. 3G–H). In Fig. 3G1–H1, denuding of the endothelium is recognized by the lack of ECs and, instead, the characteristic image of the internal elastic lamina, which is highly autofluorescent in the blue and green channels.

Quantification of endothelial bioeffects

We next wanted to quantify the extent of intracellular uptake, loss of viability and denuding present after different ultrasound exposures. We used multiple *en face* images at 40X magnification (e.g., Figs. 3B, D, F, and H) of each sample for analysis using image processing software to quantify the number of ECs that were (i) viable, (ii) viable with intracellular uptake, (iii) non-viable, and (iv) removed from the artery (presumed non-viable).

Figure 4 displays the percentage of cells in each of these four populations at low, intermediate, and high acoustic energy. The number of viable cells with intracellular uptake increased with increasing energy from the control (0% of cells) to low energy (9% of cells) to intermediate energy (24% of cells) (ANOVA, $P < 0.002$). The number of cells with intracellular uptake at the highest acoustic energy (8% of cells) decreased due to substantial loss in viability.

Figure 4 further indicates that the total number of cells present on the artery surface and the number of viable ECs decreased with increasing acoustic energy (ANOVA, $P < 0.001$ and $P < 0.001$, respectively). The difference in the total number of ECs compared to the control indicated the amount of denuding was only statistically significant at the highest acoustic energy (~67% of cells were removed, $P<0.001$). The number of viable ECs was only significantly different when comparing the high acoustic energy (~25% of cells remained viable) to the control ($P<0.004$) and comparing the intermediate energy (~82%) to the control ($P < 0.03$). The viability at the low energy (~93%) was not significantly different from the control ($P = 0.07$).

Considering drug delivery applications, these results suggest that low proportions of intracellular uptake with insignificant loss in viability can be obtained at low energies, whereas a higher proportion of intracellular uptake with some loss of viability can be achieved at intermediate energy. Finally, if a large loss of viability and significant denuding is tolerable (or desired), intracellular uptake can be achieved among remaining viable cells by applying high ultrasound energies.

Medial bioeffects

Having observed and quantified endothelial bioeffects caused by ultrasound-mediated cavitation, we next determined if cavitation had any effects deeper into arterial tissue to the SMCs present in the medial layer. In some drug delivery applications, it may be preferable to induce intracellular uptake to the underlying SMCs, such as to inhibit SMC proliferation.

By changing the focus depth of the confocal microscope, it was possible to optically slice the artery and capture images deeper in the tissue to approximately 40 μm below the endothelial surface. In Fig. 5A, the surface of an artery exposed to the highest acoustic energy was captured. Extensive denuding of the artery was evident, based on the lack of ECs and the exposure of the internal elastic lamina. Images captured deeper in the tissue, as shown in Figs. 5B–C, display SMCs that are recognized by their long and slender nuclei and orientation perpendicular to the direction of original blood flow. As indicated by propidium iodide and TO-PRO®-1 staining, SMCs in Figs. 5B–C exhibited intracellular uptake, as well as loss of viability. In

tissues exposed at lower acoustic energies, the medial layer did not show intracellular uptake or loss of viability (data not shown).

To determine if the presence of endothelial cells was a barrier to cavitation effects to smooth muscle cells, we pre-denuded arteries by rubbing the endothelial surface with a cell scraper. Confocal images from these studies (data not shown), indicated that SMC bioeffects (i.e., intracellular uptake and loss of viability) were small at low to intermediate energy and widespread at high energy, similar to Fig. 5. This result suggests that the internal elastic lamina serves as the main barrier to cavitation, and high acoustic energies are necessary to mediate intracellular uptake to SMC.

Overall these results demonstrate that bioeffects be can directed to SMCs in the medial layer of the artery; however, we expect that effects are limited to the superficial layers of the media considering the cavitation-mediated mechanism, which is expected to have limited depth penetration [25]. This treatment of SMCs may be applicable in cases where denuding of the artery is tolerable or has already occurred due to some pretreatment, such as percutaneous coronary interventions.

Intact arteries

Lastly, we wanted to determine the role of physiological conditions such as geometry, pressure, tension, or presence of blood (a higher viscosity fluid) on bioeffects induced by ultrasound exposure. To better mimic physiologic geometry and conditions, intact arteries were stretched and pressurized to approximately physiologic tension and pressure during exposure to ultrasound at the intermediate and high acoustic energies. The arteries were also filled with DMEM or whole porcine blood containing Optison® and TOPRO-1.

Figure 6A–B display representative confocal microcopy images of an intact artery filled with DMEM and exposed at the intermediate and high acoustic energies. Similarly, Fig 6C–D display representative confocal microcopy images of the endothelium of an intact artery that was filled with whole blood and exposed to ultrasound at intermediate and high acoustic energies. Intact arteries filled with either DMEM or whole blood and exposed at either energy displayed similar bioeffects to the results found in the flat artery experiments (Fig. 2) and, therefore, show that the geometry and presence of blood in a pressurized and stretched vessel did not significantly influence ultrasound exposure to cause bioeffects. Bioeffects appeared to be uniformly distributed about the circumference and not limited to the proximal or distal wall relative to the transducer. These results also suggest that the bioeffects observed may be relevant for realistic drug delivery scenarios.

DISSCUSION

Previous studies utilizing ultrasound-enhanced gene therapy have shown promising results of positive gene transfection in *ex vivo* [36] and *in vivo* [26] cardiovascular tissues. However, few studies have shown intracellular uptake of small molecules or macromolecules (e.g., proteins) for drug delivery applications in *ex vivo* or *in vivo* cardiovascular tissues [16,21]. Moreover, there is a lack of knowledge on the efficiency of this technique in terms of the number of cells affected and the relevant populations. In this study, viable *ex vivo* porcine carotid arteries were exposed to ultrasound and demonstrated the ability of this method to cause intracellular uptake of small molecules into ECs and SMCs. Furthermore, quantitative data showed the approximate energies that are relevant for drug delivery applications.

Many cardiovascular diseases and dysfunctions would benefit from a targeted means to deliver drugs or genes to the endothelium [3]. Quantitative results (Fig. 4) suggest that low to intermediate ultrasound energies would be appropriate for drug or gene delivery applications

to cause intracellular uptake or possibly transfect a large number of cells without a large loss of viability. Extensive cell death could be a drawback for drug delivery applications, since endothelial injury in the form of death or denudation could initiate an inflammation response or even thrombosis [37]. Intracellular uptake results suggest that potential applications might be limited to drug or gene delivery to a minority of the cell population, yet some gene delivery applications may not require a high transfection efficiency if the expressed protein is excreted and has a local effect. To cause intracellular uptake to the majority of the endothelium, repeated applications of ultrasound or other optimization approaches may facilitate higher uptake percentages without a harmful loss of viability. Cardiovascular diseases that could benefit from this method of targeted delivery include diseased sites such as vulnerable atherosclerotic plaques and ischemic heart or peripheral tissue. Intracellular therapeutic targets such as NADPH oxidases or gene expression of eNOS in the endothelium could help control neointimal formation and restore vascular function [3,38]. Promoting angiogenesis by intracellular delivery or gene expression agents such as VEGF or FGF in the endothelium could also benefit ischemic injuries in the myocardium or peripheral vasculature [10].

In other cases of cardiovascular disease, targeted drug or gene delivery to SMCs may be desired as is currently performed clinically with drug-eluting stents to control SMC proliferation [7] and is a goal of many gene therapy treatments [10]. We found that ultrasound exposure could also cause medial bioeffects, which were only observed at high ultrasound energies. Results suggest that cavitation is obstructed by the internal elastic lamina and limited to superficial cell layers. Intracellular uptake to SMCs might be used in applications where denuding and loss of viability is acceptable or has already occurred, such as treatment for restenosis post-angioplasty. In this potential application, extensive denuding and injury to the endothelium typically occurs from balloon inflation during percutaneous coronary interventions [37]. At this point, it may be advantageous to use ultrasound-enhanced cavitation to deliver drugs or genes to SMCs to inhibit smooth muscle proliferation and promote re-endothelialization for vascular recovery [10].

At higher ultrasound energies, extensive denuding of the endothelium was produced at the targeted site, as imaged in Fig. 3G–H and quantified in Fig. 4. A targeted loss of viability or denuding may not be desirable for drug or gene delivery applications but may be beneficial for other therapeutic applications. A number of vascular targeting agents, such as combretastatins, are currently being studied to cause EC death for anti-vascular targeting [39]. This therapy aims to selectively destroy endothelium of tumor blood vessels and subsequently cause vascular shutdown, which limits sustaining nutrients and waste removal required by the tumor [5]. High ultrasound energies focused at a tumor may be able to create this desired effect by denuding the artery.

In conclusion, this work supported the hypothesis that ultrasound-mediated cavitation can target intracellular uptake into ECs. Furthermore, we have for the first time imaged the localized patterns of intracellular uptake and shown them to be heterogeneously scattered patches that may correspond to ultrasound-mediated cavitation events. These regions of uptake and cell death often appeared to be several cells in diameter, a dimension consistent with estimates of “blast radii” from single cavitation events [18,40] and related observations of denuding cells off cultured monolayers [35]. We have also quantified the endothelial bioeffects due to ultrasound enhanced delivery and found that intracellular uptake can occur in up to 24% of ECs at intermediate ultrasound energy and that widespread denuding of ECs from the arterial surface can occur at high energy. Using intact arteries as an *ex vivo* drug delivery model, this study showed that the same bioeffects occur at near physiologic conditions. These results exhibit advantages and limitations of ultrasound-enhanced delivery that can further guide research on this technique for drug or gene delivery applications to treat cardiovascular diseases and dysfunctions.

Acknowledgements

We thank Holifield Farms for their donation of porcine tissue and laboratory members Mangesh Despande, Vladimir Zarnitsyn, Robyn Schlicher, Joshua Hutcheson, Christina Rostad and Prerona Chakravarty for their helpful discussions. This work was supported in part by the U.S. National Institutes of Health, and a fellowship to DMH from the U.S. Department of Education GAANN program. DMH and MRP are members of the Center for Drug Design, Development and Delivery and the Institute of Bioengineering and Biosciences at the Georgia Institute of Technology.

References

1. Smith SC Jr, Jackson R, Pearson TA, Fuster V, Yusuf S, Faergeman O, Wood DA, Alderman M, Horgan J, Home P, Hunn M, Grundy SM. Principles for national and regional guidelines on cardiovascular disease prevention: a scientific statement from the World Heart and Stroke Forum. Circulation 2004;109(25):3112–3121. [PubMed: 15226228]
2. Cooke JP. The endothelium: a new target for therapy. Vasc Med 2000;5(1):49–53. [PubMed: 10737156]
3. Melo LG, Gnecchi M, Pachori AS, Kong D, Wang K, Liu X, Pratt RE, Dzau VJ. Endothelium-targeted gene and cell-based therapies for cardiovascular disease. Arterioscler Thromb Vasc Biol 2004;24(10): 1761–1774. [PubMed: 15308553]
4. Cines DB, Pollak ES, Buck CA, Loscalzo J, Zimmerman GA, McEver RP, Pober JS, Wick TM, Konkle BA, Schwartz BS, Barnathan ES, McCrae KR, Hug BA, Schmidt AM, Stern DM. Endothelial cells in physiology and in the pathophysiology of vascular disorders. Blood 1998;91(10):3527–3561. [PubMed: 9572988]
5. Tozer GM, Kanthou C, Baguley BC. Disrupting tumour blood vessels. Nat Rev Cancer 2005;5(6): 423–435. [PubMed: 15928673]
6. Malecki M, Kolsut P, Proczka R. Angiogenic and antiangiogenic gene therapy. Gene Ther 2005;12 (Suppl 1):S159–169. [PubMed: 16231050]
7. Saia F, Marzocchi A, Serruys PW. Drug-eluting stents. The third revolution in percutaneous coronary intervention. Ital Heart J 2005;6(4):289–303. [PubMed: 15902927]
8. Sharif F, Daly K, Crowley J, O'Brien T. Current status of catheter- and stent-based gene therapy. Cardiovasc Res 2004;64(2):208–216. [PubMed: 15485679]
9. Baker AH, Kritz A, Work LM, Nicklin SA. Cell-selective viral gene delivery vectors for the vasculature. Exp Physiol 2005;90(1):27–31. [PubMed: 15542621]
10. Quarck R, Holvoet P. Gene therapy approaches for cardiovascular diseases. Curr Gene Ther 2004;4 (2):207–223. [PubMed: 15180587]
11. Niidome T, Huang L. Gene therapy progress and prospects: nonviral vectors. Gene Ther 2002;9(24): 1647–1652. [PubMed: 12457277]
12. Kipshidze NN, Porter TR, Dangas G, Yazdi H, Tio F, Xie F, Hellinga D, Wolfram R, Seabron R, Waksman R, Abizaid A, Roubin G, Iyer S, Colombo A, Leon MB, Moses JW, Iversen P. Novel site-specific systemic delivery of Rapamycin with perfluorobutane gas microbubble carrier reduced neointimal formation in a porcine coronary restenosis model. Catheter Cardiovasc Interv 2005;64 (3):389–394. [PubMed: 15736246]
13. Unger EC, Hersh E, Vannan M, Matsunaga TO, McCreery T. Local drug and gene delivery through microbubbles. Prog Cardiovasc Dis 2001;44(1):45–54. [PubMed: 11533926]
14. Liu Y, Miyoshi H, Nakamura M. Encapsulated ultrasound microbubbles: Therapeutic application in drug/gene delivery. J Control Release 2006;114(1):89–99. [PubMed: 16824637]
15. Suzuki R, Takizawa T, Negishi Y, Hagisawa K, Tanaka K, Sawamura K, Utoguchi N, Nishioka T, Maruyama K. Gene delivery by combination of novel liposomal bubbles with perfluoropropane and ultrasound. J Control Release. 2006
16. Mitragotri S. Healing sound: the use of ultrasound in drug delivery and other therapeutic applications. Nat Rev Drug Discov 2005;4(3):255–260. [PubMed: 15738980]
17. Leighton, TG. The Acoustic Bubble. Academic Press; London: 1994.
18. Sundaram J, Mellein BR, Mitragotri S. An experimental and theoretical analysis of ultrasound-induced permeabilization of cell membranes. Biophys J 2003;84(5):3087–3101. [PubMed: 12719239]

19. Schlicher RK, Radhakrishna H, Tolentino TP, Apkarian RP, Zarnitsyn V, Prausnitz MR. Mechanism of intracellular delivery by acoustic cavitation. Ultrasound Med Biol 2006;32(6):915–924. [PubMed: 16785013]

20. Mehier-Humbert S, Bettinger T, Yan F, Guy RH. Plasma membrane poration induced by ultrasound exposure: implication for drug delivery. J Control Release 2005;104(1):213–222. [PubMed: 15866347]

21. Bekeredjian R, Grayburn PA, Shohet RV. Use of ultrasound contrast agents for gene or drug delivery in cardiovascular medicine. J Am Coll Cardiol 2005;45(3):329–335. [PubMed: 15680708]

22. Huber PE, Mann MJ, Melo LG, Ehsan A, Kong D, Zhang L, Rezvani M, Peschke P, Jolesz F, Dzau VJ, Hynynen K. Focused ultrasound (HIFU) induces localized enhancement of reporter gene expression in rabbit carotid artery. Gene Ther 2003;10(18):1600–1607. [PubMed: 12907952]

23. Amabile PG, Waugh JM, Lewis TN, Elkins CJ, Janas W, Dake MD. High-efficiency endovascular gene delivery via therapeutic ultrasound. J Am Coll Cardiol 2001;37(7):1975–1980. [PubMed: 11401141]

24. Correas JM, Bridal L, Lesavre A, Mejean A, Claudon M, Helenon O. Ultrasound contrast agents: properties, principles of action, tolerance, and artifacts. Eur Radiol 2001;11(8):1316–1328. [PubMed: 11519538]

25. Hwang JH, Brayman AA, Reidy MA, Matula TJ, Kimmey MB, Crum LA. Vascular effects induced by combined 1-MHz ultrasound and microbubble contrast agent treatments in vivo. Ultrasound Med Biol 2005;31(4):553–564. [PubMed: 15831334]

26. Taniyama Y, Tachibana K, Hiraoka K, Namba T, Yamasaki K, Hashiya N, Aoki M, Ogihara T, Yasufumi K, Morishita R. Local delivery of plasmid DNA into rat carotid artery using ultrasound. Circulation 2002;105(10):1233–1239. [PubMed: 11889019]

27. Hashiya N, Aoki M, Tachibana K, Taniyama Y, Yamasaki K, Hiraoka K, Makino H, Yasufumi K, Ogihara T, Morishita R. Local delivery of E2F decoy oligodeoxynucleotides using ultrasound with microbubble agent (Optison) inhibits intimal hyperplasia after balloon injury in rat carotid artery model. Biochem Biophys Res Commun 2004;317(2):508–514. [PubMed: 15063786]

28. Mukherjee D, Wong J, Griffin B, Ellis SG, Porter T, Sen S, Thomas JD. Ten-fold augmentation of endothelial uptake of vascular endothelial growth factor with ultrasound after systemic administration. J Am Coll Cardiol 2000;35(6):1678–1686. [PubMed: 10807476]

29. Chesler NC, Conklin BS, Hand HC, Ku DN. Simplified ex vivo artery culture techniques for porcine arteries. J Vasc Invest 1998;4:123–127.

30. Kamaev PP, Hutcheson JD, Wilson ML, Prausnitz MR. Quantification of optison bubble size and lifetime during sonication dominant role of secondary cavitation bubbles causing acoustic bioeffects. J Acoust Soc Am 2004;115(4):1818–1825. [PubMed: 15101659]

31. Klibanov AL. Targeted delivery of gas-filled microspheres, contrast agents for ultrasound imaging. Adv Drug Deliv Rev 1999;37(1–3):139–157.

32. Hallow DM, Mahajan AD, McCutchen TE, Prausnitz MR. Measurement and correlation of acoustic cavitation with cellular bioeffects. Ultrasound Med Biol 2006;32(7):1111–1122. [PubMed: 16829325]

33. Acoustical Society of America, ANSI Technical Report: Bubble Detection and Cavitation Monitoring 2002.

34. Brayman AA, Lizotte LM, Miller MW. Erosion of artificial endothelia in vitro by pulsed ultrasound: acoustic pressure, frequency, membrane orientation and microbubble contrast agent dependence. Ultrasound Med Biol 1999;25(8):1305–1320. [PubMed: 10576273]

35. Ohl CD, Wolfrum B. Detachment and sonoporation of adherent HeLa-cells by shock wave-induced cavitation. Biochim Biophys Acta 2003;1624(1–3):131–138. [PubMed: 14642823]

36. Teupe C, Richter S, Fisslthaler B, Randriamboavonjy V, Ihling C, Fleming I, Busse R, Zeiher AM, Dimmeler S. Vascular gene transfer of phosphomimetic endothelial nitric oxide synthase (S1177D) using ultrasound-enhanced destruction of plasmid-loaded microbubbles improves vasoreactivity. Circulation 2002;105(9):1104–1109. [PubMed: 11877363]

37. Davis C, Fischer J, Ley K, Sarembock IJ. The role of inflammation in vascular injury and repair. J Thromb Haemost 2003;1(8):1699–1709. [PubMed: 12911580]

38. Ray R, Shah AM. NADPH oxidase and endothelial cell function. Clin Sci (Lond) 2005;109(3):217–226. [PubMed: 16104842]

39. Thorpe PE. Vascular targeting agents as cancer therapeutics. Clin Cancer Res 2004;10(2):415–427. [PubMed: 14760060]

40. Guzman HR, McNamara AJ, Nguyen DX, Prausnitz MR. Bioeffects caused by changes in acoustic cavitation bubble density and cell concentration: a unified explanation based on cell-to-bubble ratio and blast radius. Ultrasound Med Biol 2003;29(8):1211–1222. [PubMed: 12946524]

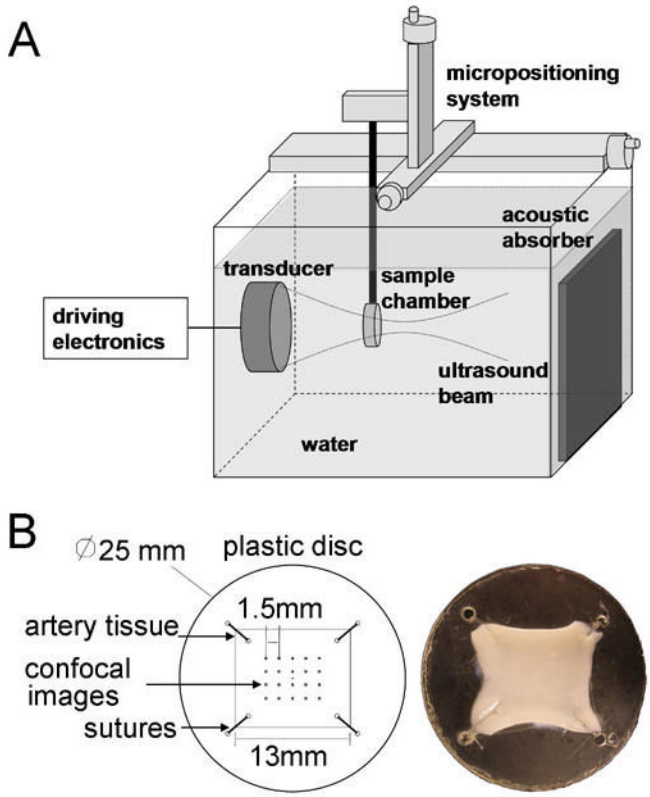

Figure 1.
(A) Equipment schematic (B) Artery segments were sutured to TPX® plastic disks exposing the endothelium for flat artery experiments. Confocal images for quantification of bioeffects were captured in a 5×4 array, where each image was spaced by 1.5 mm.

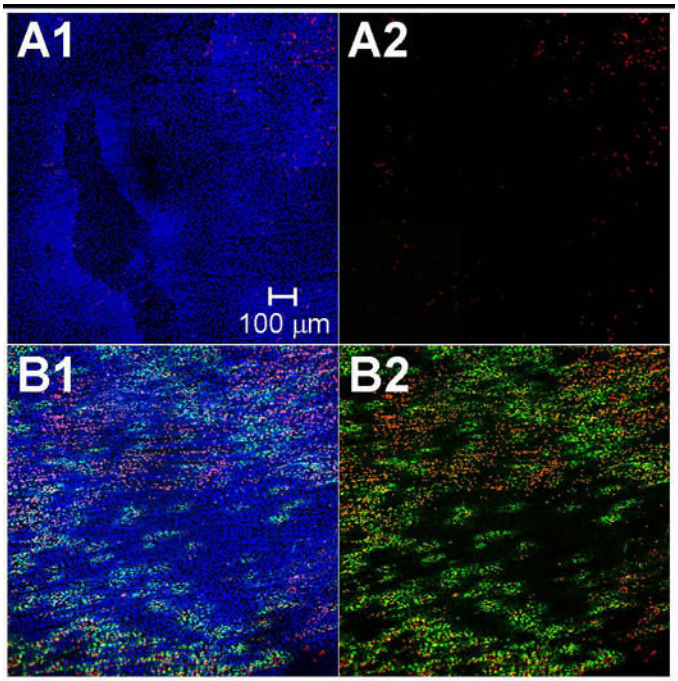

Figure 2.

Confocal microscopy 2×2 image montages (10X magnification) displaying the localization of intracellular uptake enhanced by ultrasound. Images depict the endothelium of (A) a control sample and (B) a sample exposed to intermediate ultrasound energy. EC nuclei were labeled with Hoechst 33342 (blue) to stain all cells, propidium iodide (red) to stain dead cells, and TO-PRO®-1 (green) to indicate intracellular uptake. (A2) and (B2) are shown without blue fluorescence to more clearly view intracellular uptake and cell death.

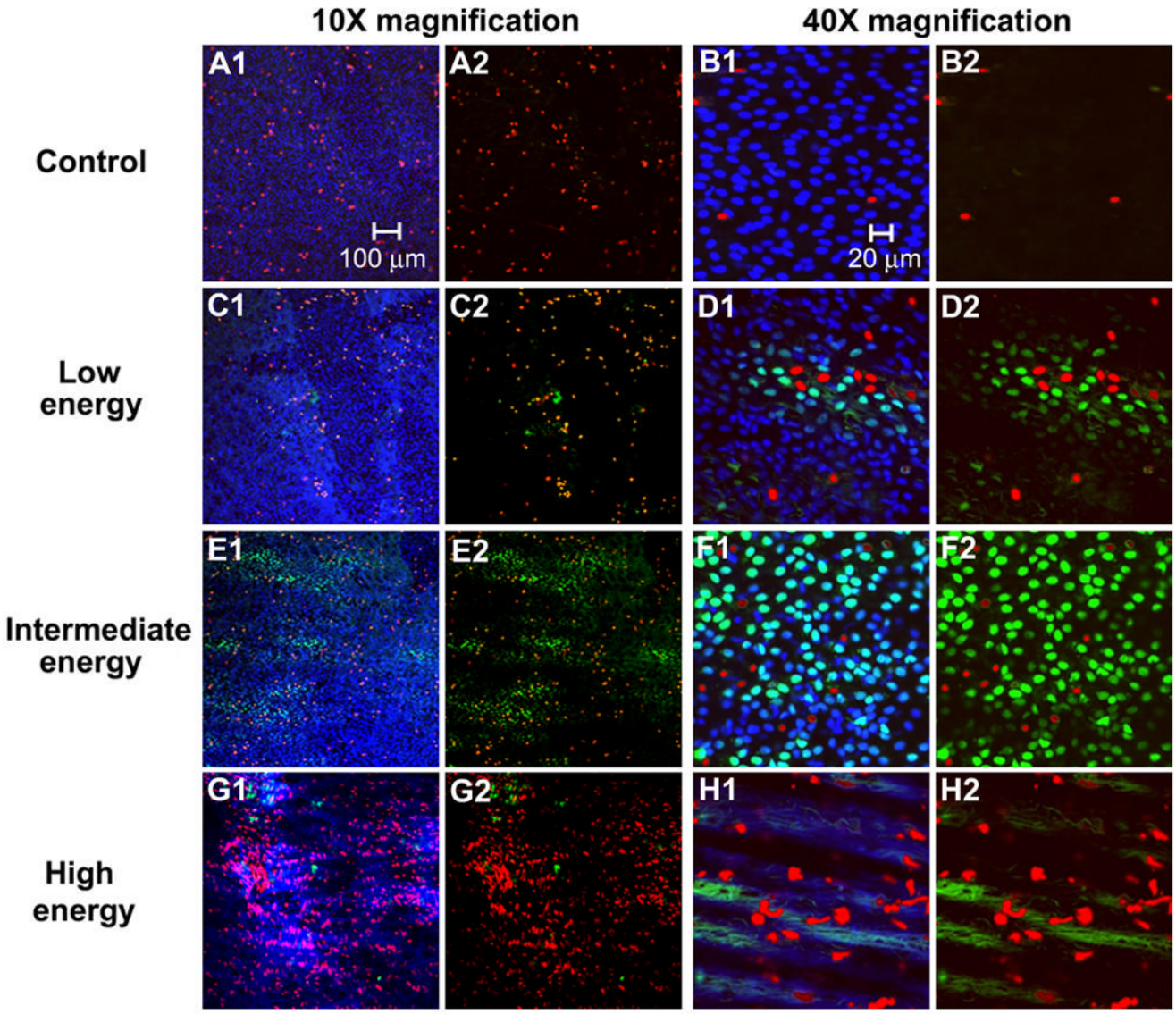

Figure 3.

Confocal microscopy images of the artery surface at 10X (A, C, E, G) and 40X magnification (B, D, G, H) showing the range of bioeffects at different ultrasound energies. Images depict (A–B) a control sample and samples exposed to ultrasound at (C–D) low, (E–F) intermediate, and (G–H) high energies. Figures A2–H2 are shown without blue fluorescence to more clearly view intracellular uptake and cell death.

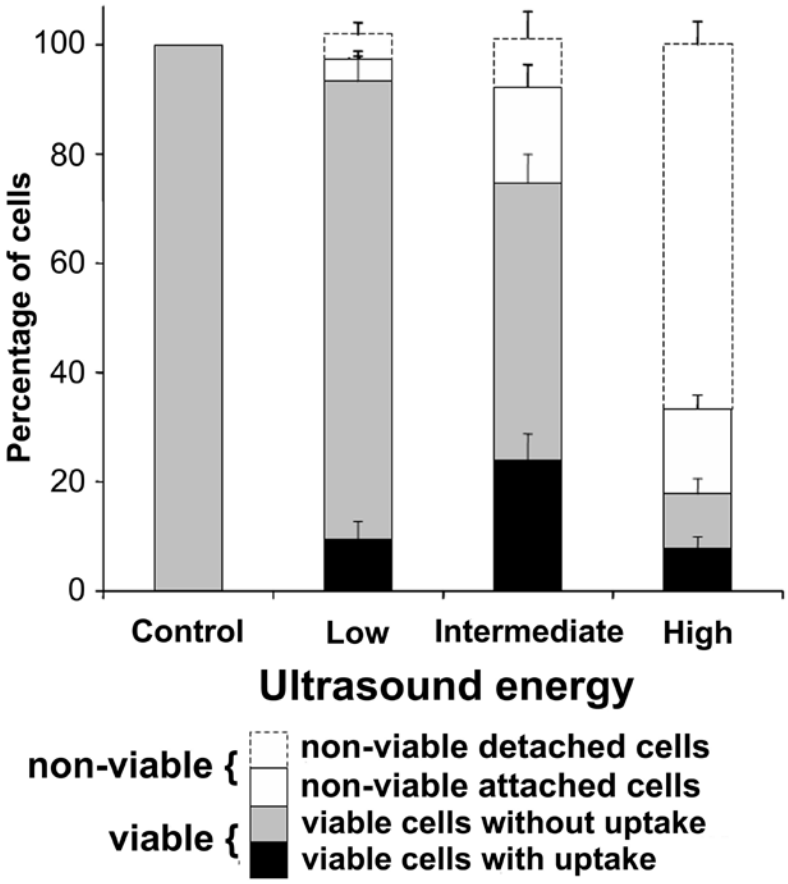

Figure 4.
Quantification of endothelial bioeffects following ultrasound exposure. Data represent the averages of $n \geq 5$ replicates with SEM shown.

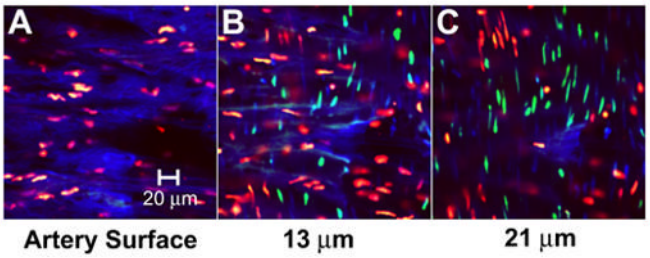

Figure 5.
Confocal microscopy images at multiple depths in the artery displaying bioeffects to medial SMCs. Images were captured at (A) the artery surface and (B) 13 μm and (C) 21 μm below the artery surface.

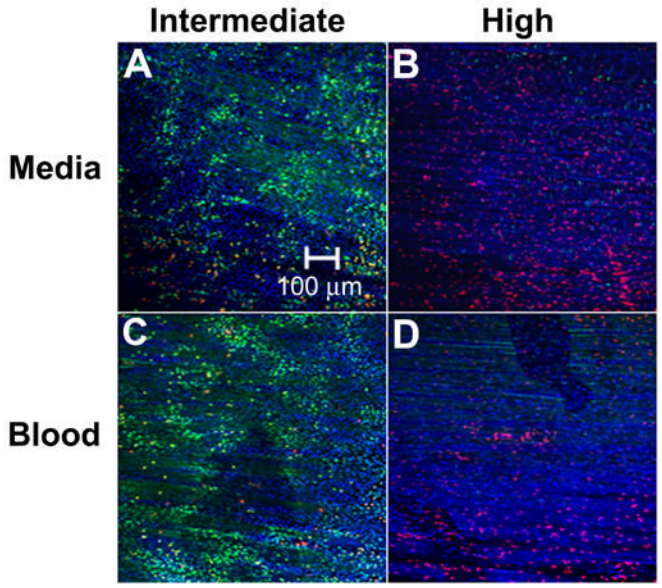

Figure 6.

Confocal microscopy images of endothelium displaying bioeffects mediated by ultrasound exposure to intact arteries at near physiologic conditions. Ultrasound was applied at (A, C) intermediate and (B, D) high energy while the artery was filled with (A, B) DMEM or (C, D) blood.